JACS
JOURNAL OF THE AMERICAN CHEMICAL SOCIETY
Cite This: J. Am. Chem. Soc. 2019, 141, 5092−5096
Communication
pubs.acs.org/JACS

Synthesis of Type I PbSe/CdSe Dot-on-Plate Heterostructures with Near-Infrared Emission

Kali R. Williams,[†] Benjamin T. Diroll,[‡] Nicolas E. Watkins,[†] Xue Rui,[§] Alexandra Brumberg,[†] Robert F. Klie,[§] and Richard D. Schaller*[,†,‡]

[†]Department of Chemistry, Northwestern University, Evanston, Illinois 60208, United States
[‡]Center for Nanoscale Materials, Argonne National Laboratory, Lemont, Illinois 60439, United States
[§]Department of Physics, University of Illinois at Chicago, Chicago, Illinois 60607, United States

Supporting Information

ABSTRACT: Zero-dimensional PbSe quantum dots are heterogeneously nucleated and grown onto two-dimensional zincblende CdSe nanoplatelets. Electron microscopy shows ad-grown dots predominantly decorate edges and corners of the nanoplatelets. Spectroscopic characterizations relate type I electronic alignment as demonstrated via photoluminescence excitation spectroscopy enhancement of near-infrared emission. Transient photoluminescence and absorption convey ultrafast transfer of excitons to the lower energy semiconductor dots. These structures combine benefits of large absorption cross sections of nanoplatelets and efficient near-infrared emission of PbSe with quantum confinement tuning of energy gap.

Heterostructured nanocrystals offer synthetically tunable routes to control the nature of electronic excitations beyond what is possible with size and shape alone in single component materials.[1] Type I semiconductor heterostructures in particular, which localize the electron and hole to the same component, are frequently employed to confine excitations for enhanced photoluminescence[2] (PL) which is a critical property in applications such as bioimaging,[3] single photon sources,[4] color conversion,[5] light-emitting diodes,[6] and luminescent solar concentrators.[7] Thus far, variation in composition and heterostructure morphology have been relatively limited for colloidal nanoplatelets (NPLs). As a class of materials, NPLs are of interest due to precise synthetic control allowing for no dispersion in thickness,[8,9] nascent control over lateral extent,[10] large absorption cross sections,[11,12] efficient and exceptionally narrow optical emission,[9] polarized optical properties,[13−15] and amplified spontaneous emission and lasing with low thresholds and high gain.[10,11,16]

NPL heterostructures have primarily focused on adaptations of core/shell structures, such as CdSe/ZnS, CdSe/CdS, CdS/ZnS, deposited using standard high-temperature ad-growth methods[17] and more recent colloidal atomic layer deposition.[18,19] Further synthetic work has been performed to change the optical properties while retaining the original thickness, such as via alloy tuning and core-crown morphologies of both type I and type II electronic structure, but have tended to remain, with rare exception,[20] in the visible optical window.[21−24] In recent work, ad-growth of quasi-spherical nanoparticles of different compositions onto NPLs has been reported for metallic Au, Pt, and Pd on CdSe NPLs[25,26] as well as wide gap ZnSe semiconductor quantum dots (QDs).[27]

Here, we investigate ad-growth of a smaller band gap semiconductor nanomaterial, PbSe, which offers type I heterostructuring that should yield funneling of excitations from the large absorption cross-section NPL into the QDs. Conditions are developed that yield PbSe QDs grown on CdSe NPLs using a seeded-growth hot-injection method.[28,29] PbSe, in particular, is chosen for ad-growth because the lattice parameters of the cubic CdSe and PbSe phases are closely matched and this composition is well-known to afford high emission quantum yield PbSe/CdSe core/shell heterostructures.[30,31] On the other hand, cation exchange of these compositions has also been reported at elevated temperatures—this is the most common method for synthesis of core/shells—but exchange of cadmium by lead requires excess lead, elevated temperature (>130 °C), and prolonged exposure times (e.g., 1 h).[32]

Ad-growth of PbSe QDs onto CdSe NPLs coarsely followed earlier hot injection protocols that target PbSe QD products,[33,34] but with important modifications to prevent both homogeneous nucleation via reduction of achieved supersaturation as well as Pb for Cd cation exchange reactions. CdSe NPL substrates were first synthesized following literature procedures.[2] Changes made to suppress homogeneous nucleation include smaller precursor amounts of lead (100 μmol versus 2 mmol) and selenium (0.1 M versus 1 M), reduction of injection temperatures from 170 to 180 to 130 °C, utilization of higher purity phosphine precursor solution (97% TOP versus 90%) that contains fewer dialkylphosphine impurities,[35] and short reactions times (3 min). This combination of conditions helps to both push kinetics in favor of heterogeneous nucleation and suppress cation exchange as noted below. For example, reactions performed under typical conditions for PbSe QD synthesis yielded a reaction product dominated by PbSe QDs rather than heterostructures (Figure S1). Additionally, because some homogeneous nucleation is still observed under these more favorable reaction conditions, the desired materials were isolated via size selective precipitation[36] by adding minimal

Received: December 27, 2018
Published: March 18, 2019

DOI: 10.1021/jacs.8b13794
J. Am. Chem. Soc. 2019, 141, 5092−5096

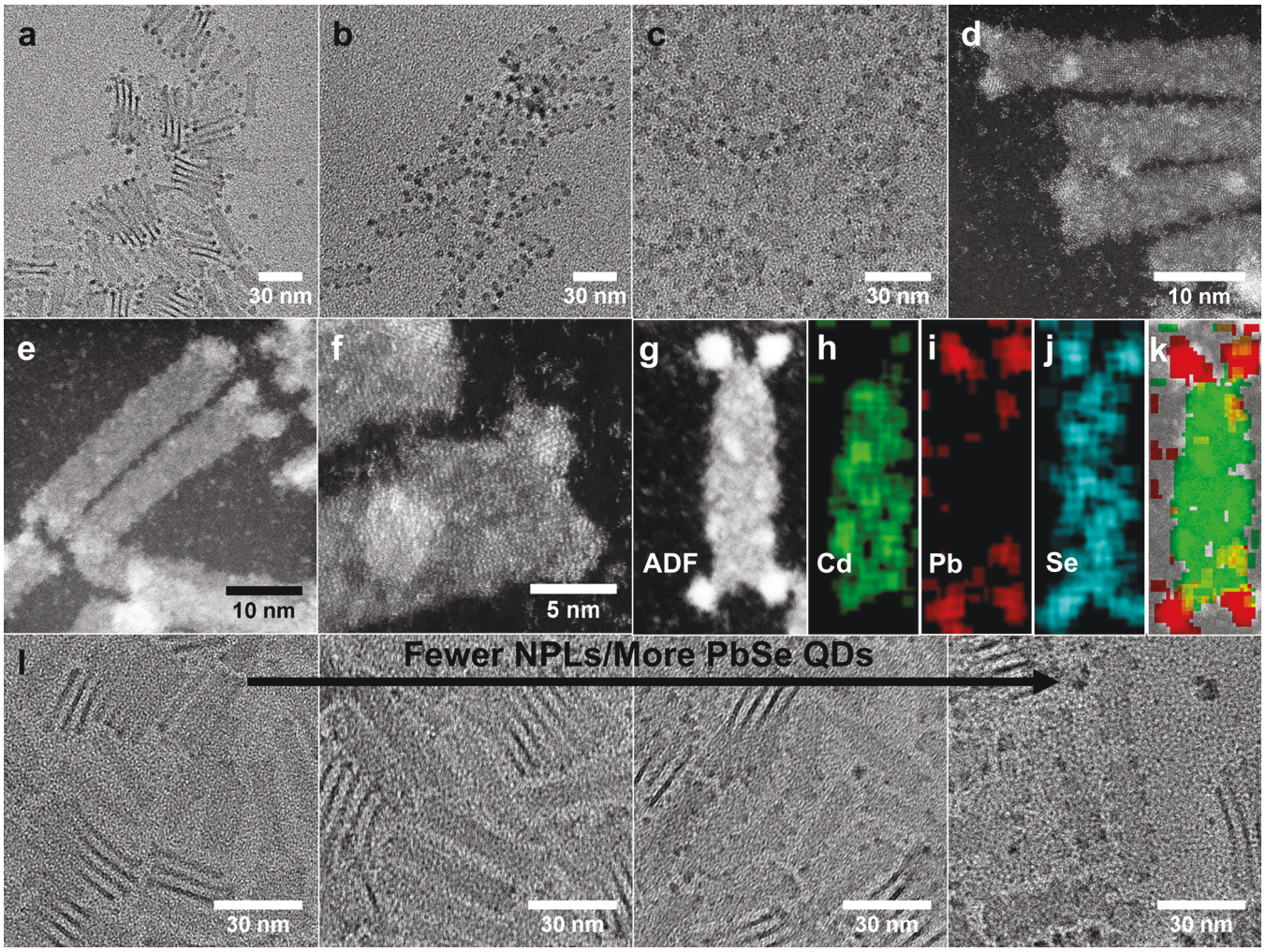

Figure 1. Bright-field TEM micrographs of PbSe/CdSe dot-on-plate heterostructures synthesized with (a, b) 5 ML CdSe NPL seeds and (c) 4 ML NPL seeds. (d–f) HAADF-STEM micrographs of a PbSe/CdSe dot-on-plate heterostructure. (g) Annular dark field image of PbSe/CdSe dot-on-plate heterostructure with corresponding EDX maps of (h) cadmium, (i) lead, and (j) selenium. (k) Merged image of ADF, cadmium, and lead maps. (l) Series of reaction products with decreasing NPL injection concentration, showing increasing PbSe QD decoration.

amounts of isopropanol antisolvent and centrifuging for 30 min at 8000 r.p.m.. This procedure separated the desired PbSe dot-on-plate heterostructures from homogeneously nucleated PbSe QDs.

The resulting heterostructures present a dot-on-plate morphology similar in form to related reports[25−27] which is apparent in transmission electron microscopy (TEM) images. Figure 1a,b shows PbSe/CdSe dot-on-plate heterostructures formed with 5 ML CdSe NPLs and Figure 1c shows similar structures formed with 4 ML CdSe NPLs. High-angle annular dark-field scanning transmission electron microscopy (HAADF-STEM) measurements of PbSe/5 ML CdSe NPL heterostructures in Figure 1d–f shows the bright PbSe dots, which scatter substantially more electrons to the high-angle annular detector, distinct from the CdSe NPLs. A single PbSe/5 ML CdSe NPL heterostructure is shown in the HAADF-STEM image in Figure 1g followed by elemental maps of cadmium, lead, and selenium collected by energy dispersive X-ray (EDX) spectroscopy in Figure 1h–j. The merged image in Figure 1k confirms the preserved composition of the CdSe NPL and the ad-growth of PbSe dots decorating the NPL corners (see also Figure S2 for elemental mapping). X-ray diffraction data (Figure S3) is also consistent with the addition of crystalline PbSe QDs to the NPLs.

The preponderance of PbSe QDs nucleate as spherical shapes on the corners and edges of the NPLs, although some do appear to nucleate on the flat NPL planes. This is largely consistent with the understanding concerning NPL growth, in which high energy penalties are associated with homoepitaxy on the flat surfaces, leading to two-dimensional growth.[37,38] An additional measure of control in this synthesis is provided by tuning the concentration of NPLs in the PbSe growth medium: at lower NPL concentrations, the number of PbSe nuclei per NPL increases, with more decoration of the edge of the NPL after corner sites are saturated. An example is shown in Figure 1l, which shows the progression of reaction products for a series of reactions conducted with decreasing NPL concentrations. Still, in all experiments, it is noteworthy that decoration of CdSe NPLs by PbSe remained nonconformal in an apparent regime of Volmer–Weber type islands. Given the excellent lattice match of the two crystals and the existence of core/shell heterostructures of this composition, the limited wetting of PbSe on CdSe is somewhat surprising and may be related to particular challenges of epitaxy on the atomically flat

DOI: 10.1021/jacs.8b13794
J. Am. Chem. Soc. 2019, 141, 5092−5096

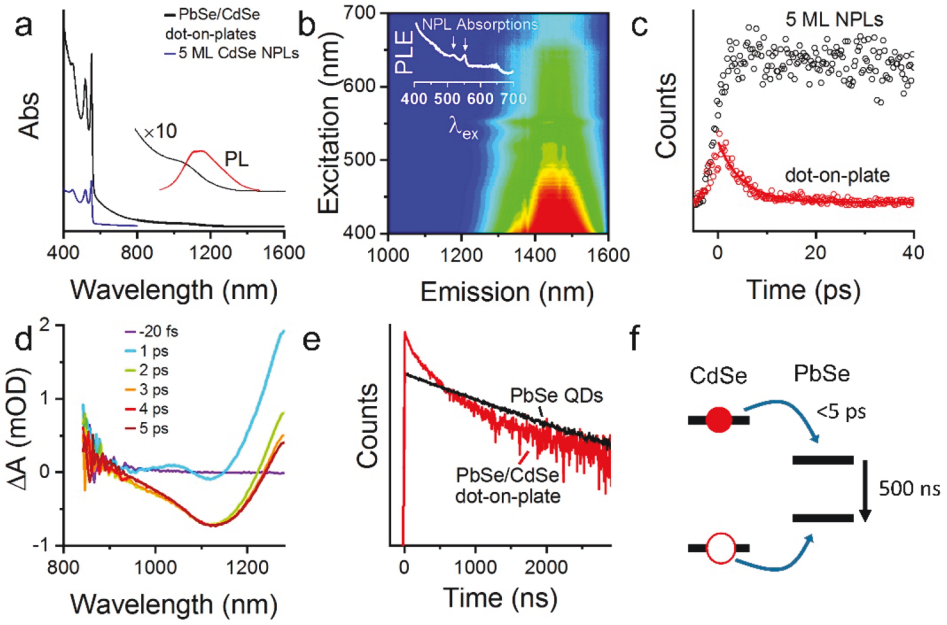

Figure 2. (a) Absorption (solid black line) and photoluminescence (red line) of typical PbSe/CdSe dot-on-plate heterostructures. The solid blue line shows the absorption spectrum of the 5 ML CdSe NPL seeds. (b) Photoluminescence excitation (PLE) map of the emission in the NIR for visible excitation wavelengths of a PbSe/CdSe dot-on-plate heterostructure emitting at 1450 nm. Inset shows the integrated counts in the visible with the features of the 5 ML NPL absorption apparent in the excitation spectrum. (c) Visible time-resolved photoluminescence of a PbSe/CdSe dot-on-plate heterostructure at early time, shown in red dots, compared to the time-resolved photoluminescence of the 5 ML CdSe NPL seed, shown in black circles. A solid fit line represents an exponential decay fit of the dot-on-plate PL data with a lifetime of 4.9 ps. (d) Transient absorption spectra of the a PbSe/CdSe dot-on-plate heterostructure showing early time dynamics. (e) Time-resolved photoluminescence of the PbSe/CdSe dot-on-plate heterostructure collected to longer delay times, compared with time-resolved photoluminescence of a PbSe QD sample of comparable band gap. (f) Schematic of the type 1 heterostructure model developed from the experimental data.

NPLs, which are not present in spherical structures, or effects of ligand crowding following PbSe nucleation.

Spectroscopic measurements are consistent with the findings of the presented structural observations. UV−vis and FTIR measurements (Figure 2a) further show excitonic absorption features that resemble those of isolated CdSe NPLs (here an excitonic absorption at 550 nm for 5 ML NPLs) and PbSe QDs, which display an excitonic absorption feature at 1050 nm in this case. The preserved sharpness of the visible absorption features of the NPLs is particularly noteworthy as prior reports involving the synthesis of heterostructures frequently resulted in substantial broadening of absorption resonances,[18,27] suggesting that the heterostructures formed here do not experience a substantial change in the strain or electron−phonon coupling of the NPL. Furthermore, retention of CdSe NPL features supports that negligible Pb for Cd cation exchange occurs. Matching the NIR absorption resonance of the PbSe component is the emission from the sample, centered at 1150 nm, representing a large quasi-Stokes shift from the dominant NPL absorption. A substantial advantage of this type of heterostructure is the large increase in the absorption oscillator strength in the visible.

Direct comparison with PbSe QDs of comparable size to those decorating the NPLs suggests that the PbSe/CdSe dot-on-plate structures have a minimum of five times stronger absorption strength at visible wavelengths shorter than the absorption resonances of the 5 ML NPLs used as seeds (Figure S4). This underlines the strong enhancement of absorption conferred by the CdSe NPL.

Several measurements were performed to evaluate electronic interaction between the two components of the heterostructure. As shown in Figure 2b, photoluminescence excitation spectra (PLE) detecting NIR emission for a typical PbSe/CdSe dot-on-plate sample shows the characteristic absorption resonances of the CdSe NPLs in the PLE of the PbSe QDs. Time-resolved measurements confirm that this is not arising from efficient reabsorption of NPL emission and instead comes from the rapid transfer of excitations in the NPL to the PbSe QDs in a type I structure. With visible excitation of the heterostructures, visible emission from the heterostructures at the CdSe band-edge is ∼0.1% of the intensity for similar optical density unaltered NPLs (Figure S5). Whereas the room temperature lifetime of isolated NPLs is typically in the nanosecond range,[9] the decay of NPL PL from dot-on-plate heterostructures apparent in time-resolved measurements shown in Figure 2c is rapid (∼5 ps in these measurements). This rapid quenching of photoemission is a strong indication of electron and/or hole transfer to the PbSe.[39] Because the visible PL counts in Figure 2c decrease to approximately 0, nearly every NPL in the heterostructure ensemble likely has a QD attached to it. Further, NIR transient absorption measurements in Figure 2d and Figure S6a indicate a 620 fs relaxation time into the excitonic state of the PbSe of dot-on-plate heterostructures, which is measurably slower than intraband cooling in pure PbSe QDs (190 fs, Figure S6b).

Static emission quantum yields also suggest that transfer of excitations is rapid: PbSe/CdSe heterostructures gave estimated quantum yields of 16−17%, comparable to freshly prepared IV−VI QDs, for both 450 and 808 nm excitation. Whereas emission from the CdSe NPL in the heterostructure is quenched rapidly, emission from the PbSe QDs decorating the NPLs shows approximately normal dynamics for small

DOI: 10.1021/jacs.8b13794
J. Am. Chem. Soc. 2019, 141, 5092−5096

PbSe QDs (Figure 2e), albeit with some trapping. The measured emission lifetime is 497 ± 8 ns versus 1200 ns for isolated PbSe QDs with a similar excitonic absorption energy. The combined static and time-resolved PL data indicate that the PbSe/CdSe dot-on-plate heterostructures have a type I electronic structure, shown in the scheme in Figure 2f: the exciton created in the decorated NPLs transfers rapidly to a QD, which subsequently displays band-edge PL.

In conclusion, this work reports the seeded-growth synthesis of PbSe/CdSe dot-on-plate heterostructures with near IR emission. These materials show fast and efficient funneling of excitations from the CdSe NPL to the PbSe QDs characteristic of a type I heterostructure. Such dot-on-plate heterostructures facilitate large effective Stokes shifts, boost the effective absorption cross section of the IR-emitting QD, lower the local symmetry of the PbSe particles, and display IR emission comparable to other available semiconductor QDs.

■ ASSOCIATED CONTENT

Supporting Information

Supporting Information.pdf The Supporting Information is available free of charge on the ACS Publications website at DOI: 10.1021/jacs.8b13794.

Experimental details and additional spectroscopic data (PDF)

■ AUTHOR INFORMATION

Corresponding Author

*schaller@anl.gov; schaller@northwestern.edu

ORCID

Benjamin T. Diroll: 0000-0003-3488-0213
Alexandra Brumberg: 0000-0003-2512-4686
Richard D. Schaller: 0000-0001-9696-8830

Notes

The authors declare no competing financial interest.

■ ACKNOWLEDGMENTS

We acknowledge support from National Science Foundation DMREF Program under award DMR-1629383 and by the National Science Foundation Graduate Research Fellowship Program under Grant No. DGE-1324585 (N.E.W., A.B.). Use of the Center for Nanoscale Materials, an Office of Science user facility, was supported by the U.S. Department of Energy, Office of Science, Office of Basic Energy Sciences, under Contract No. DE-AC02-06CH11357. Use of the JEOL JEM-ARM200CF in the Electron Microscopy Core of UIC's Research Resource Center was supported by grants from the National Science Foundation (DMR-0959470 and DMR-1626065).

■ REFERENCES

(1) Reiss, P.; Protière, M.; Li, L. Core/Shell Semiconductor Nanocrystals. *Small* **2009**, *5*, 154−168.
(2) Hines, M. A.; Guyot-Sionnest, P. Synthesis and Characterization of Strongly Luminescing ZnS-Capped CdSe Nanocrystals. *J. Phys. Chem.* **1996**, *100*, 468−471.
(3) Bruchez, M., Jr. Semiconductor Nanocrystals as Fluorescent Biological Labels. *Science* **1998**, *281*, 2013−2016.
(4) Mahler, B.; Spinicelli, P.; Buil, S.; Quelin, X.; Hermier, J.-P.; Dubertret, B. Towards Non-Blinking Colloidal Quantum Dots. *Nat. Mater.* **2008**, *7*, 659−664.
(5) Coe-Sullivan, S.; Liu, W.; Allen, P.; Steckel, J. S. Quantum Dots for LED Downconversion in Display Applications. *ECS J. Solid State Sci. Technol.* **2013**, *2*, R3026−R3030.
(6) Colvin, V. L.; Schlamp, M. C.; Alivisatos, A. P. Light-Emitting Diodes Made from Cadmium Selenide Nanocrystals and a Semiconducting Polymer. *Nature* **1994**, *370*, 354−357.
(7) Klimov, V. I.; Baker, T. a.; Lim, J.; Velizhanin, K. a.; McDaniel, H. Quality Factor of Luminescent Solar Concentrators and Practical Concentration Limits Attainable with Semiconductor Quantum Dots. *ACS Photonics* **2016**, *3*, 1138−1148.
(8) Ithurria, S.; Dubertret, B. Quasi 2D Colloidal CdSe Platelets with Thicknesses Controlled at the Atomic Level. *J. Am. Chem. Soc.* **2008**, *130*, 16504−16505.
(9) Ithurria, S.; Tessier, M. D.; Mahler, B.; Lobo, R. P. S. M.; Dubertret, B.; Efros, A. L. Colloidal Nanoplatelets with Two-Dimensional Electronic Structure. *Nat. Mater.* **2011**, *10*, 936−941.
(10) She, C.; Fedin, I.; Dolzhnikov, D. S.; Dahlberg, P. D.; Engel, G. S.; Schaller, R. D.; Talapin, D. V. Red, Yellow, Green, and Blue Amplified Spontaneous Emission and Lasing Using Colloidal CdSe Nanoplatelets. *ACS Nano* **2015**, *9*, 9475−9485.
(11) She, C.; Fedin, I.; Dolzhnikov, D. S.; Demortière, A.; Schaller, R. D.; Pelton, M.; Talapin, D. V. Low-Threshold Stimulated Emission Using Colloidal Quantum Wells. *Nano Lett.* **2014**, *14*, 2772−2777.
(12) Achtstein, A. W.; Antanovich, A.; Prudnikau, A.; Scott, R.; Woggon, U.; Artemyev, M. Linear Absorption in CdSe Nanoplates: Thickness and Lateral Size Dependency of the Intrinsic Absorption. *J. Phys. Chem. C* **2015**, *119*, 20156−20161.
(13) Cunningham, P. D.; Souza, J. B.; Fedin, I.; She, C.; Lee, B.; Talapin, D. V. Assessment of Anisotropic Semiconductor Nanorod and Nanoplatelet Heterostructures with Polarized Emission for Liquid Crystal Display Technology. *ACS Nano* **2016**, *10*, 5769−5781.
(14) Scott, R.; Heckmann, J.; Prudnikau, A. V.; Antanovich, A.; Mikhailov, A.; Owschimikow, N.; Artemyev, M.; Climente, J. I.; Woggon, U.; Grosse, N. B.; Achtstein, A. W. Directed Emission of CdSe Nanoplatelets Originating from Strongly Anisotropic 2D Electronic Structure. *Nat. Nanotechnol.* **2017**, *12*, 1155−1160.
(15) Ma, X.; Diroll, B. T.; Cho, W.; Fedin, I.; Schaller, R. D.; Talapin, D. V.; Wiederrecht, G. P. Anisotropic Photoluminescence from Isotropic Optical Transition Dipoles in Semiconductor Nanoplatelets. *Nano Lett.* **2018**, *18*, 4647−4652.
(16) Guzelturk, B.; Kelestemur, Y.; Olutas, M.; Delikanli, S.; Demir, H. V. Amplified Spontaneous Emission and Lasing in Colloidal Nanoplatelets. *ACS Nano* **2014**, *8*, 6599−6605.
(17) Mahler, B.; Nadal, B.; Bouet, C.; Patriarche, G.; Dubertret, B. Core/Shell Colloidal Semiconductor Nanoplatelets. *J. Am. Chem. Soc.* **2012**, *134* (45), 18591−18598.
(18) Ithurria, S.; Talapin, D. V. Colloidal Atomic Layer Deposition (c-ALD) Using Self-Limiting Reactions at Nanocrystal Surface Coupled to Phase Transfer between Polar and Nonpolar Media. *J. Am. Chem. Soc.* **2012**, *134*, 18585−18590.
(19) Diroll, B. T.; Talapin, D. V.; Schaller, R. D. Violet-to-Blue Gain and Lasing from Colloidal CdS Nanoplatelets: Low-Threshold Stimulated Emission Despite Low Photoluminescence Quantum Yield. *ACS Photonics* **2017**, *4*, 576−583.
(20) Izquierdo, E.; Robin, A.; Keuleyan, S.; Lequeux, N.; Lhuillier, E.; Ithurria, S. Strongly Confined HgTe 2D Nanoplatelets as Narrow Near-Infrared Emitters. *J. Am. Chem. Soc.* **2016**, *138*, 10496−10501.
(21) Pedetti, S.; Ithurria, S.; Heuclin, H.; Patriarche, G.; Dubertret, B. Type-II CdSe/CdTe Core/Crown Semiconductor Nanoplatelets. *J. Am. Chem. Soc.* **2014**, *136*, 16430−16438.
(22) Tessier, M. D.; Spinicelli, P.; Dupont, D.; Patriarche, G.; Ithurria, S.; Dubertret, B. Efficient Exciton Concentrators Built from Colloidal Core/Crown CdSe/CdS Semiconductor Nanoplatelets. *Nano Lett.* **2014**, *14*, 207−213.
(23) Dufour, M.; Steinmetz, V.; Izquierdo, E.; Pons, T.; Lequeux, N.; Lhuillier, E.; Legrand, L.; Chamarro, M.; Barisien, T.; Ithurria, S. Engineering Bicolor Emission in 2D Core/Crown CdSe/$CdSe_{1-x}Te_x$ Nanoplatelet Heterostructures Using Band-Offset Tuning Engineering Bicolor Emission in 2D Core/Crown CdSe/$CdSe_{1-x}Te_x$ Nano-

DOI: 10.1021/jacs.8b13794
J. Am. Chem. Soc. 2019, 141, 5092−5096

platelet Heterostructures Using Band-Offset Tuning. *J. Phys. Chem. C* **2017**, *121*, 24816−24823.
(24) Yadav, S.; Singh, A.; Sapra, S. Long-Lived Emission in Type-II CdS/ZnSe Core/Crown Nanoplatelet Heterostructures. *J. Phys. Chem. C* **2017**, *121*, 27241−27246.
(25) Naskar, S.; Schlosser, A.; Miethe, J. F.; Steinbach, F.; Feldhoff, A.; Bigall, N. C. Site-Selective Noble Metal Growth on CdSe Nanoplatelets. *Chem. Mater.* **2015**, *27*, 3159.
(26) Mahler, B.; Guillemot, L.; Bossard-Giannesini, L.; Ithurria, S.; Pierucci, D.; Ouerghi, A.; Patriarche, G.; Benbalagh, R.; Lacaze, E.; Rochet, F.; Lhuillier, E. Metallic Functionalization of CdSe 2D Nanoplatelets and Its Impact on Electronic Transport. *J. Phys. Chem. C* **2016**, *120*, 12351−12361.
(27) Yadav, S.; Adhikary, B.; Tripathy, P.; Sapra, S. E Ffi Cient Charge Extraction from CdSe/ZnSe Dots-on-Plates Nanoheterostructures. *ACS Omega* **2017**, *2*, 2231−2237.
(28) Carbone, L.; Nobile, C.; De Giorgi, M.; Sala, F. D.; Morello, G.; Pompa, P.; Hytch, M.; Snoeck, E.; Fiore, A.; Franchini, I. R.; Nadasan, M.; Silvestre, A. F.; Chiodo, L.; Kudera, S.; Cingolani, R.; Krahne, R.; Manna, L. Synthesis and Micrometer-Scale Assembly of Colloidal CdSe/CdS Nanorods Prepared by a Seeded Growth Approach. *Nano Lett.* **2007**, *7*, 2942−2950.
(29) Talapin, D. V.; Nelson, J. H.; Shevchenko, E. V.; Aloni, S.; Sadtler, B.; Alivisatos, A. P. Seeded Growth of Highly Luminescent CdSe/CdS Nanoheterostructures with Rod and Tetrapod Morphologies. *Nano Lett.* **2007**, *7*, 2951−2959.
(30) Pietryga, J. M.; Werder, D. J.; Williams, D. J.; Casson, J. L.; Schaller, R. D.; Klimov, V. I.; Hollingsworth, J. A. Utilizing the Lability of Lead Selenide to Produce Heterostructured Nanocrystals with Bright, Stable Infrared Emission. *J. Am. Chem. Soc.* **2008**, *130*, 4879−4885.
(31) Zhang, Y.; Dai, Q.; Li, X.; Cui, Q.; Gu, Z.; Zou, B.; Wang, Y.; Yu, W. W. Formation of PbSe/CdSe Core/Shell Nanocrystals for Stable Near-Infrared High Photoluminescence Emission. *Nanoscale Res. Lett.* **2010**, *5*, 1279−1283.
(32) Lee, D.; Kim, W. D.; Lee, S.; Bae, W. K.; Lee, S.; Lee, D. C. Direct Cd-to-Pb Exchange of CdSe Nanorods into PbSe/CdSe Axial Heterojunction Nanorods. *Chem. Mater.* **2015**, *27*, 5295−5304.
(33) Yu, W. W.; Falkner, J. C.; Shih, B. S.; Colvin, V. L. Preparation and Characterization of Monodisperse PbSe Semiconductor Nanocrystals in a Noncoordinating Solvent. *Chem. Mater.* **2004**, *16*, 3318−3322.
(34) Murray, C. B.; Sun, S.; Gaschler, W.; Doyle, H.; Betley, T. a.; Kagan, C. R. Colloidal Synthesis of Nanocrystals and Nanocrystal Superlattices. *IBM J. Res. Dev.* **2001**, *45*, 47−56.
(35) Steckel, J. S.; Yen, B. K. H.; Oertel, D. C.; Bawendi, M. G. On the Mechanism of Lead Chalcogenide Nanocrystal Formation. *J. Am. Chem. Soc.* **2006**, *128*, 13032−13033.
(36) Murray, C. B.; Norris, D.; Bawendi, M. G. Synthesis and Characterization of Nearly Monodisperse CdE (E= S, Se, Te) Semiconductor Nanocrystallites. *J. Am. Chem. Soc.* **1993**, *115*, 8706−8715.
(37) Riedinger, A.; Ott, F. D.; Mule, A.; Mazzotti, S.; Knüsel, P. N.; Kress, S. J. P.; Prins, F.; Erwin, S. C.; Norris, D. J. An Intrinsic Growth Instability in Isotropic Materials Leads to Quasi-Two-Dimensional Nanoplatelets. *Nat. Mater.* **2017**, *16*, 743−748.
(38) Ott, F. D.; Riedinger, A.; Ochsenbein, D. R.; Knüsel, P. N.; Erwin, S. C.; Mazzotti, M.; Norris, D. J. Ripening of Semiconductor Nanoplatelets. *Nano Lett.* **2017**, *17*, 6870−6877.
(39) Diroll, B. T.; Turk, M. E.; Gogotsi, N.; Murray, C. B.; Kikkawa, J. M. Ultrafast Photoluminescence from the Core and the Shell in CdSe/CdS Dot-in-Rod Heterostructures. *ChemPhysChem* **2016**, *17*, 759−765.

DOI: 10.1021/jacs.8b13794
J. Am. Chem. Soc. 2019, 141, 5092−5096